THE TRISTRON, A NEW PARADIGM IN HIGH-EFFICIENCY RF POWER GENERATION

I. Syratchev †, N. Catalan Lasheras, R. Gerard, L. Giezendanner, R. Leuxe, C. Marrelli, W.L. Millar, A. Piccini, A. S. Thakur, European Organization for Nuclear Research, Geneva, Switzerland
G. Burt, Z. Un Nisa, Lancaster University, Lancaster, UK

Abstract

The tristron concept was proposed many years ago but it was never developed to a stage where it could be mass produced. Based on IOTs technology, the tristron promises to achieve RF efficiency above 90 % for a wide frequency and power range. Building on the development of high-efficiency klystrons, CERN is proposing this new device as the power source of choice for the Future Circular Collider (FCC_{ee}). This paper will focus on the conceptual design of the tristron and outline the development being carried out at CERN.

INTRODUCTION

For the FCC_{ee}, high efficiency in converting grid electricity to RF power is a top priority, along with keeping RF power sources cost-effective and compact.

Over the past five years, CERN's High Efficiency Klystron project has developed a new concept: a compact (3 m tall), low-voltage (< 60 kV) Two-Stage Multi-Beam klystron (TS MBK) [1]. This device can produce continuous RF power up to 1.2 MW at 400 MHz with efficiency above 85%. The design is complete and ready for industrial prototyping. The simulated TS MBK performance is shown in Fig. 1. The novel TS MBK technology can also be considered as an optimal choice for the different High Energy colliders such as CLIC, ILC and MC [2].

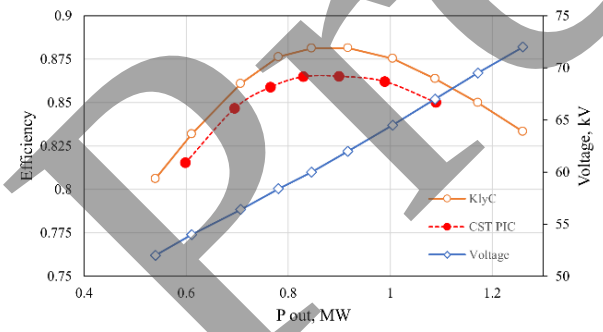

Figure 1: The simulated RF power/efficiency performance of the TS MBK operated at different high voltage levels.

At the time of this development, it was established that for the Z, W/H, and tt̄ stages, one tube would power one, two, and eight cavities, respectively. Recent evolution of the FCC_{ee} RF system with a double gap 400 MHz SRF cavity reduces the maximum RF power needed for a single cavity from 1 MW to below 0.5 MW for Z, W and H poles. For the Z pole, Reverse Phase Operation regime (RPO) [3] is proposed in which the accelerating cavities are divided into two families —focusing and defocusing— with different RF power transient modulation to compensate for the beam abort gap (Fig. 2). As a result, a single 0.5 MW RF power source feeding one cavity satisfies all the operating energies. Following these changes, the TS MBK design was scaled down from 1 MW to 0.5 MW while maintaining its original high efficiency. With the required RF power modulation, the klystron will operate below saturation most of the time, reducing its efficiency from 85% (at saturation) to about 67%.

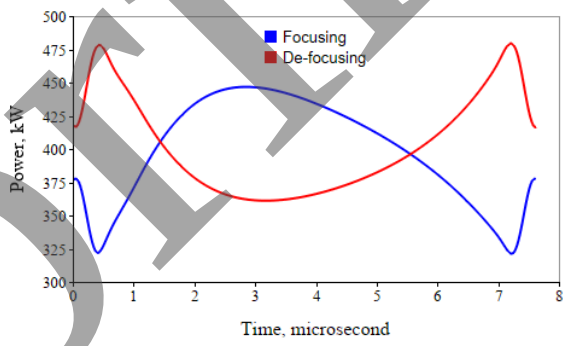

Figure 2: The transient RF power modulation profiles for the two families of accelerating cavities (Z-pole). The average power is 400 kW.

TRISTRON CONCEPT

Gridded tubes, such as the Inductive Output Tube (IOT) [4], are another class of electrovacuum devices known for operating efficiently over a wide range of RF output power levels when controlled by the input RF signal. A 1.2 MW, 0.7 GHz multi-beam (10-beam) IOT was successfully prototyped for ESS nearly a decade ago [5], demonstrating that high-power multi-beam IOT technology is mature. However, its practical efficiency was limited to about 70%.

An extended IOT version, called "Tristron" (hybrid of triode and klystron) was originally proposed in the late 1960s [6], but it was never commercialized. The tristron comprises an additional idler cavity located before the output cavity, which dramatically improves the bunching quality and increases efficiency from 70 % to above 90 %. Such an improvement is based on several key technical and conceptual elements, which are outlined below.

The ***multi-beam technology*** is a common approach for high power and high efficiency vacuum tubes. In this configuration the total beam current is divided into individual beamlets. Thus, beam perveance ($K=I/V^{1.5}$) is attributed to

†igor.syratchev@cern.ch

the individual beam. While studying the FCC_{ee} TS MBK output RF cavity driven by ideal bunches, we found that the ultimate efficiency reach follows the trend:

$$\eta = 0.94 - 0.16 \times \mu K \quad . \qquad (1)$$

The IOT input RF cavity, with a ***gridded gun***, naturally produces saturated bunches because cathode emission is suppressed when the RF field in the cathode–grid gap is negative. However, the bunches formed and accelerated across the high voltage grid–anode gap are monoenergetic. As a result, the power extraction efficiency in the output cavity is limited to about 75 % for Class B operation (with a bunch length of 180° RF phase), which is typical for commercial IOTs.

The ***penultimate cavity*** is the key new component in the tristron's RF circuit compared to the IOT. As monoenergetic bunches passing through it, they experience velocity modulation, whose amplitude (called congregation) depends on the cavity frequency detuning. During propagation through the drift tube toward the output cavity, these bunches undergo compression, as shown in Fig. 3. This process is very similar to that in a klystron's bunching circuit, where initial velocity modulation is converted into current density modulation (bunching) along the device. By optimizing the positive detuning of the penultimate cavity and the drift tube length, the bunch quality can be brought close to the ideal case in terms of length and congregation, increasing the overall efficiency from 75% to about 85%.

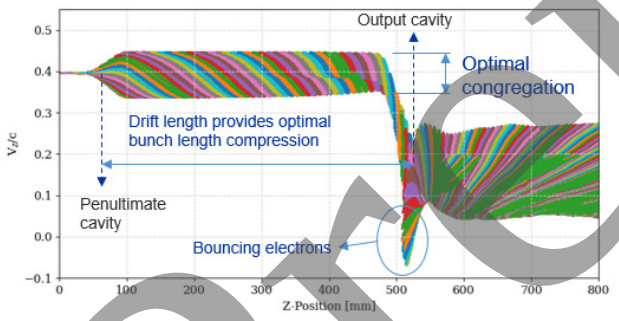

Figure 3: Particles velocity along the tristron simulated in CST 3D PIC. Different colours represent different time steps in simulation.

Another efficiency improvement comes from the controlled ***manipulation of the bouncing electrons*** negative velocities in the output cavity, see Fig. 3. This is done by optimising the output cavity parameters like negative frequency detuning, cavity gap length and external Q factor. In turn, this increases the tube efficiency further from 85 % to about 90 %.

Finally, ***hollow beams*** were adopted to reduce bunch stratification, i.e., the radial variation in bunch length that develops as the bunch propagates along the drift tube. This provided an additional 2 % increase in efficiency, raising it to about 92 %, which is close to the theoretical maximum efficiency given in Eq. (1) for a tube with a microperveance of 0.1 $\mu A/V^{1.5}$.

FCC_{ee} 0.4 GHz, 0.5MW, CW MULTIBEAM TRISTRON

Our initial design approach for the FCC_{ee} MB tristron was to scale the topology of the existing ESS MB IOT to a lower frequency and add an idler cavity to the RF circuit. However, after assessing the complexity of such a device, with 10 individual input RF cavities (one per beamlet) requiring precise synchronization of resonant frequencies, RF phases, and voltages—we opted for a different solution. In this configuration, a common input cavity hosts all cathodes, reducing both the size and cost of the RF circuit.

A further simplification concerns the gridded cathode design. Unlike the spherical cathodes with electrostatic focusing (beam compression) typically used in conventional IOTs, we chose a flat cathode–grid assembly without beam compression. This choice simplifies the beam optics, as cathodes themselves are embedded in the constant magnetic field provided by the external solenoid.

Design parameters of the FCC_{ee} 400 MHz, CW MB tristrons are summarized in Table 1. Following this, we provide a brief overview of the tristron by subsystem.

Table 1: Parameters of the FCC_{ee} 400 MHz MB Tristron

Parameter	Value
Voltage, kV	46
Total current, A	10.7
N beams	10
Microperveance, $\mu A/V^{1.5}$	0.11
Efficiency, %	>90
Power, kW	>440

Gridded Gun

The gridded gun is one of the most critical components of the tristron. Its design follows general recommendations for the operating frequency range, including a grid–cathode spacing of 0.3 mm and a grid wire cross-section of 0.15 mm × 0.15 mm.

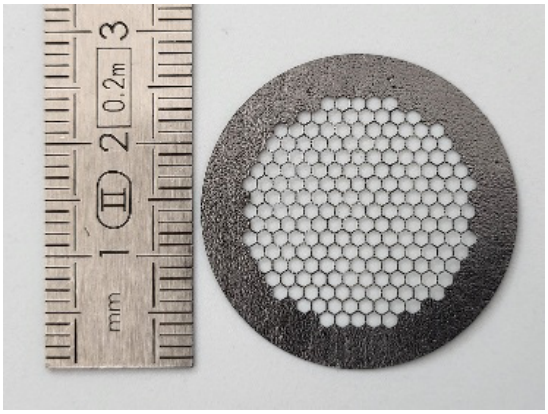

Figure 4: An image of the flat HEX grid fabricated at CERN using Laser-cut technology on a PG wafer.

Pyrolytic graphite (PG) was selected as the grid material, following a common practice in modern high-power gridded tubes. A hexagonal grid topology (HEX grid), shown

in Fig. 4, was chosen due to its superior heat removal capacity compared to other configurations.

The tristron RF circuit design requires accurate knowledge of the bunch length and shape produced in the actual gun environment. To achieve this, we developed advanced simulation methods for gridded guns [7]. As an example, snapshots of a bunch propagating through the system are shown in Fig. 5. The bunched current envelopes at different positions, measured by current monitors, are shown in Fig. 6, while the transient beam power intercepted by the grid is shown in Fig. 7. The simulations were performed using the commercial software CST Particle Studio.

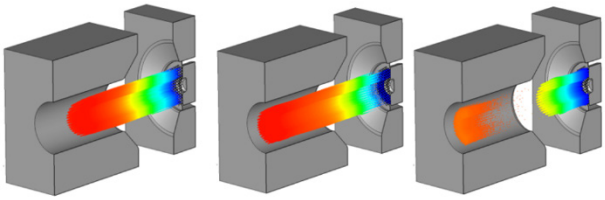

Figure 5: Simulated bunch propagation along the gun at different time steps.

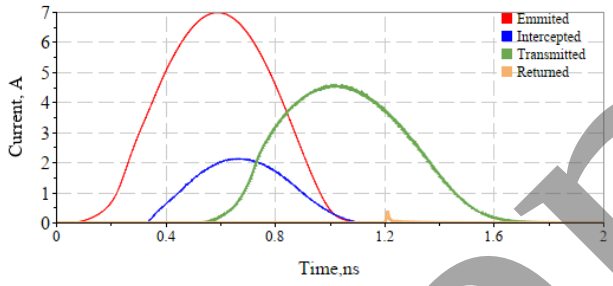

Figure 6: Bunch's current envelopes at different positions measured by current monitors. The average transmitted current is 1.07 A.

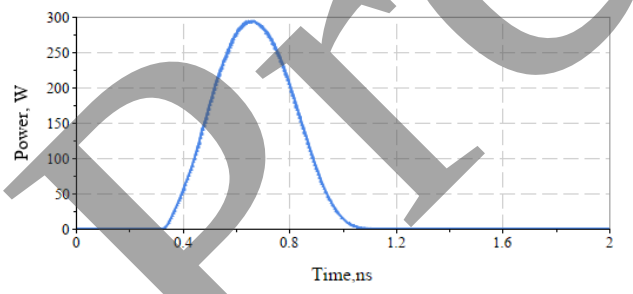

Figure 7: The transient beam power intercepted by the grid. The average dissipated power on the grid is 56.8 W.

Together with black body radiation from the cathode operating at 1000 °C, the beam power losses were used for thermomechanical and stress analysis of the grid using ANSYS software. Temperature-dependent material properties were included, along with accurate modelling of thermal conductance at the clamped interface between the grid and its support. The ambient temperature of the grid support structure was set to 100 °C. Under these conditions, the maximum grid temperature reached 426 °C, with a maximum principal stress of 11.2 MPa and a minimum principal stress of −0.3 MPa. Grid deformation in any direction did not exceed 2 µm. The temperature distribution across the grid is shown in Fig. 8.

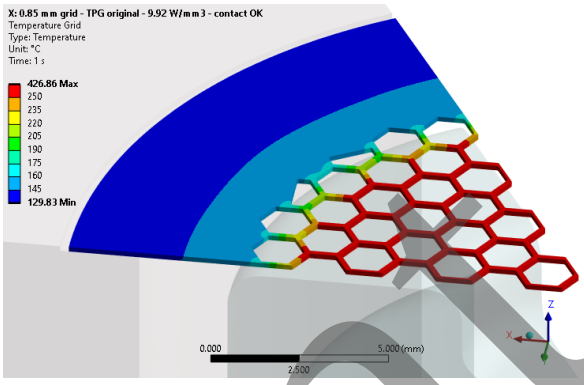

Figure 8: Map of the temperature distribution on the grid.

Input Cavity

To avoid the current emission from the cathode, when the input RF signal is inhibited, the grid is operated at some biased potential with respect to the cathode voltage. The amplitude of this bias voltage depends on the ratio between the cathode–grid and grid–anode gaps, the cathode voltage, and the grid's opacity to the electric field. For the gridded gun described above, a DC blocking voltage of 165 V is required to suppress the current.

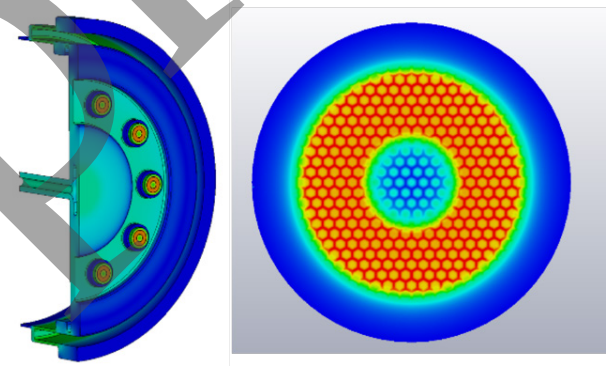

Figure 9: Electric field in the tristron's input cavity (left) and detail of the electric field in the gap between the cathode and the grid (right).

As far as grided guns themselves are part of the input cavity resonant volume, the cavity must be designed in a way so that its volume stays 'closed' for the RF field but provides discontinuity for the DC current. This is achieved using an RF choke, i.e., a resonant reflecting RF circuit that behaves as an RF short circuit without requiring direct electrical contact. The electric field distribution in the tristron input cavity designed with this approach is shown in Fig. 9, together with a detail view of the RF field in the cathode–grid gap. By design, the choke rejector ensures very low RF radiation leakage from the cavity, corresponding to an external quality factor $Q_{ext} > 2 \times 10^5$. A capacitive "doorknob" coaxial coupler is placed at the cavity centre, providing $Q_{ext} = 150$. The cavity operates in the TM_{020} mode.

MB Tristron RF Circuit

Using the bunched beam data from the gridded gun simulations, the tristron RF circuit was optimized with CERN's in-house klystron code KlyC [8]. The tube performance operated at different high-voltage settings is summarized in Fig. 10, which shows only the maximum efficiency points for each setpoint. Overall, the tristron can achieve high efficiency (>80 %) over an RF power range from 150 kW to 600 kW by selecting the appropriate operating voltage.

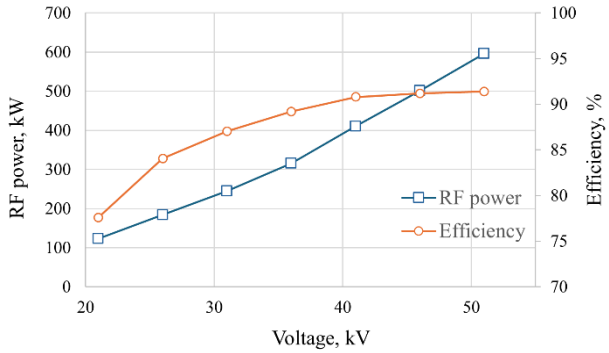

Figure 10: Maximal efficiency (squares) and RF output power (circles) of the tristron at different high voltage setting.

Next, the 3D model of the tristron RF circuit was generated in CST and tuned according to the KlyC results. The tube was excited by bunched beams at 400 MHz. In these simulations, electron bunch profiles were taken directly from CST gridded gun simulations and imported into CST PIC 3D simulations of the RF circuit with beam. A snapshot of particle propagation through the system is shown in Fig. 11.

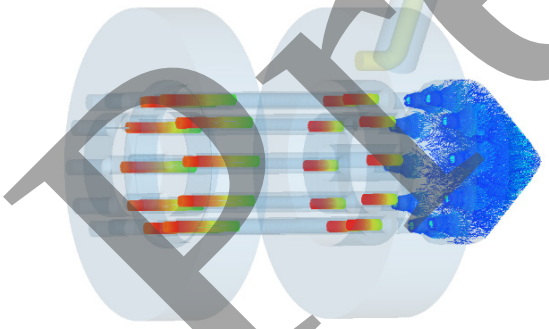

Figure 11: Electrons propagating along the tristron as simulated by CST. Colours represent particle velocities.

Measuring very high efficiency in a numerical environment is challenging. In CST PIC simulations, the extracted RF power is often reported at the output coupler port, but in our experience this value is sensitive to mesh density and does not always converge easily. An alternative approach is to evaluate the power of the spent beam in the collector and compute the tube's electronic efficiency accordingly:

$$\eta_e = \frac{P_{in} - P_{COLLECTOR}}{P_{in}}. \qquad (2)$$

Here P_{in} is the power of the incoming beam. For consistency, we have also measured this power directly in dedicated PIC simulations by absorbing the beam before the input cavity. Now, the RF power balanced efficiency can be calculated by including the Ohmic efficiency in the output RF cavity:

$$\eta_{RF} = \eta_e \times \left(1 - \frac{Q_{ext}}{Q_0}\right) \quad . \qquad (3)$$

This method appeared to be rather insensitive to the mesh density. The tristron performance at 46 kV obtained from CST PIC simulations is compared to the KlyC results in Fig. 12. Notably, at lower power levels CST predicts higher efficiency than KlyC. This can be explained by the fact that the KlyC model uses rectangular bunches with fixed length, whereas in the gridded gun the effective bunch length depends on the average beam current—the lower the current, the shorter the bunch [7]. In interaction with the penultimate cavity, lower-current bunches experience reduced congregation, which improves efficiency at lower currents.

At the design point of 46 kV and 10.7 A total beam current, CST simulations predict a balanced efficiency of 90.5 % (446 kW), which is in a good agreement with the target tristron parameters in Table 1. For comparison, efficiency evaluated from direct RF power measurements at the coupler port yields 93.5 % (456 kW), leaving some ambiguity in the exact value. The tristron efficiency–power characteristic shown in Fig. 12 was then used to estimate the operational efficiency for the FCC_{ee} RPO regime (cf. Fig. 2), resulting in 88.2 %.

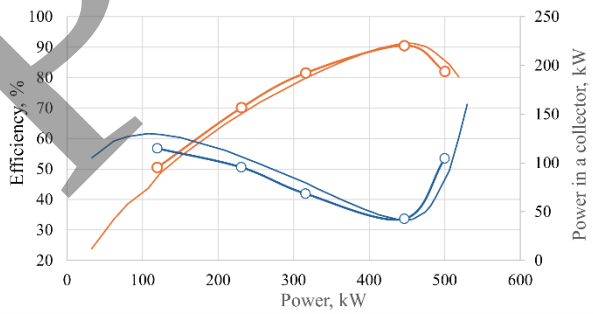

Figure 12: The MB tristron efficiency (orange) and power in the collector (blue) vs. output RF power. CST results (circles) and KlyC results (thin solid line) are shown.

Collector

To reduce complexity and fabrication cost, we adopted a common collector design, which absorbs the spent beam power from individual beamlets on a shared surface, as shown in Fig. 11. The collector design takes advantage of the fact that in standby mode, when no RF is applied, no beam is present in the system. However, for a fixed high-voltage setting, the power deposited in the collector depends on the output RF power level (see Fig. 12). The collector geometry was therefore optimized for the operating point with the highest spent-beam power load, corresponding to 100 kW of output RF power.

The interface between the multiple drift tubes and the common collector was carefully engineered to prevent backscattering of reflected electrons at the highest-efficiency operating point, where some spent beam electrons have relatively low velocity. Over the full output RF power range, the peak power density on the collector surface reaches about 120 W/cm², which remains well below the 200 W/cm² limit typically used in industrial vacuum tube collector design.

DC Breaker

The DC breaker is a specialised RF component that is transparent to microwave signals but blocks DC current. It is required in the gridded tube to enable RF priming of the input RF cavity, operated at high voltage, from an external RF driver. Our DC breaker design is based on a resonant cavity with a very low external Q factor and a choke-based resonant rejector, as shown in Fig. 13. At the −3 dB transmission level, the device provides a 30 MHz bandwidth, with ohmic insertion losses of −0.04 dB at the operating frequency.

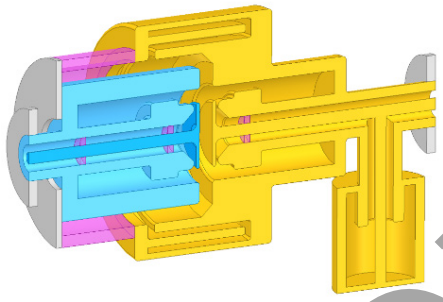

Figure 13: Artistic view of the coaxial DC breaker. Here, the input port (blue colour) is at ground potential and output port (yellow colour) is at HV potential. Insulating HV ceramic is shown in pink.

RF Window

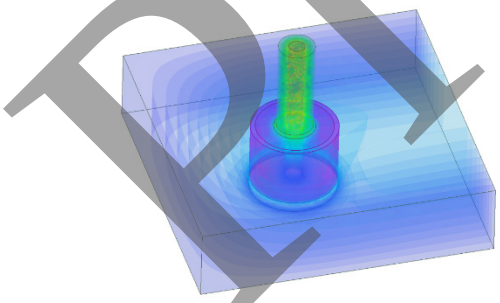

Figure 14: RF window topology showing the RF electrical field as a coloured map. Ceramic tube is shown in pink

The RF ceramic window is required to isolate the tube vacuum from the external atmosphere. It must reliably transmit up to 0.5 MW of continuous-wave RF power at 400 MHz. We adopted a robust and cost-effective solution consisting of an 18 cm diameter alumina (Al_2O_3) ceramic tube insulator with a 10 mm wall thickness.

The insulator is integrated into a half-height standard WR2300 waveguide used in the 400 MHz FCC_{ee} RF network, so no additional waveguide taper is required. The ceramic tube itself also acts as a matching element in the coaxial-to-waveguide transition, as shown in Fig. 14. At −30 dB reflection level, the window provides a 10 MHz bandwidth. At the operating frequency, RF losses in the ceramic are about 10 W for 0.5 MW of transmitted RF power, with a maximum electric field on the ceramic surface of 150 kV/m.

External Solenoid

An external solenoid is used to confine the individual beamlets within the drift tubes along the tristron RF circuit. It consists of seven main coils generating a longitudinal magnetic field of 0.08 T. At the upstream end, the magnetic circuit is closed by a ferromagnetic pole piece with ten openings, one for each beam.

An upstream correction coil is used to fine-tune the magnetic field uniformity in the cathode region, while a downstream correction coil controls the field in the collector region, where it is adjusted to be close to 0 T. Beam tracking simulations in CST 3D showed that beam scalloping (radial oscillation of the beam envelope) remains below ±1.5 % along the tube. The total solenoid power consumption is 5.1 kW.

The integrated FCC_{ee} 400 MHz MB tristron layout with the external solenoid is shown in Fig. 15.

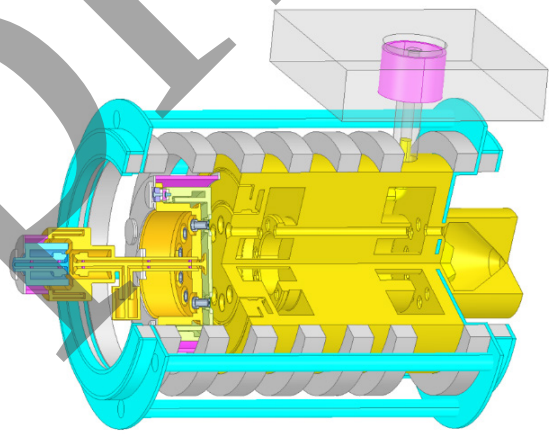

Figure 15: Artistic view of the FCC_{ee} 400 MHz MB Tristron with external solenoid. Magnetic circuit is shown in blue, and coils are shown in grey.

CONCLUSION

The MB tristron is now selected as the baseline 400 MHz, 0.5 MW CW RF power source for the FCC_{ee} [9]. It offers high operational efficiency (close to 90%), a compact footprint (1.4 m high and 1 m in diameter), and a cost-efficient design. The MB tristron is currently under development as a CERN internal project, with the first prototype expected to be built and tested at CERN in 2028.

The MB tristron parameters, as presented here, are compatible with installation in the Large Hadron Collider with minor modifications, while providing higher RF power with lower wall-plug power. It could also be a technology of choice for improving the overall efficiency of high-intensity, high-power proton SRF linacs such as European Spallation Source and MYRRHA.

REFERENCES

[1] N. Catalan-Lasheras *et al.*, "High-efficiency klystrons from a dream to a reality", in *Proc. of 15th International Particle Accelerator Conference (IPAC'24)*, Nashville, TN, USA, May 2024, pp. 3933-3938. doi:10.18429/jacow-ipac2024-fryd1

[2] J. Cai and I. Syratchev, "Modelling and Technical Design Study of Two-Stage Multibeam Klystron for CLIC*", IEEE Trans. Electron Devices*, vol. 67, no. 8, Aug. 2020. doi:10.1109/ted.2020.3000191

[3] I. Karpov *et al.*, "FCC-ee RF operation scenarios - new baseline", presented at FCC week 2025, Viena, Austria, May 2025.

[4] A. Haeff, "An Ultra-High-Frequency Power Amplifier of Novel Design", *Electronics*, Feb. 1939, pp. 30-32.

[5] M. Jensen *et al.*, "Testing of the ESS MB-IOT prototypes", in *Proc. IPAC'18*, Vancouver, Canada, Apr.-May 2018, pp. 1759-1764. doi:10.18429/JACoW-IPAC2018-WEXGBF1

[6] A.D. Sushkov and V.K. Fedyaev, "Electrons bunching simulations in triode-klystron (tristron)," Izvestiya Vuzov, *Radioelectronics*, vol. 10, no11, pp. 1033, 1969 [in Russian].

[7] A. S. Thakur *et al.*, "Design of an RF gridded gun for high efficiency Triston", presented at the IPAC'26, Deauville, France, May 2026, paper MOP7192, this conference.

[8] J. Cai and I. Syratchev, "KlyC: 1.5-D Large-Signal Simulation Code for Klystrons", *IEEE Trans. Plasma Sci.*, vol. 47, no. 4, pp. 1734-1741, Apr. 2019. doi:10.1109/tps.2019.2904125

[9] M. Benedict *et al.*, "Future Circular Collider Feasibility Study Report Volume 2: Accelerators, technical infrastructure and safety", CERN-FCC-ACC-2025-0004, Geneva, Switzerland, Mar. 2025. doi:10.1140/epjs/s11734-025-01967-4